

UNCLASSIFIED

AD 416468

DEFENSE DOCUMENTATION CENTER

FOR

SCIENTIFIC AND TECHNICAL INFORMATION

CAMERON STATION, ALEXANDRIA, VIRGINIA



UNCLASSIFIED

NOTICE: When government or other drawings, specifications or other data are used for any purpose other than in connection with a definitely related government procurement operation, the U. S. Government thereby incurs no responsibility, nor any obligation whatsoever; and the fact that the Government may have formulated, furnished, or in any way supplied the said drawings, specifications, or other data is not to be regarded by implication or otherwise as in any manner licensing the holder or any other person or corporation, or conveying any rights or permission to manufacture, use or sell any patented invention that may in any way be related thereto.

416 468

AD No. —

DDC FILE COPY

①

SEP 13 1963
RECEIVED
TISIA B

416 468

ANTENNA AND RADIO WAVE PROPAGATION
CHARACTERISTICS AT VHF NEAR AND IN THE GROUND

APPROVED:

A. H. LaGrone

A. W. Straiton

(5) 868 500

(6) (5-9) M

ANTENNA AND RADIO WAVE PROPAGATION
CHARACTERISTICS AT VHF NEAR AND IN THE GROUND

by

(10)

by Douglas M. Schwartz, BSEE

Air Force Institute of Technology

BS Educ., Texas Christian University

(12) 45p.

(13-15) NA

THESIS

(16-17) AA

Presented to the Faculty of the Graduate School of

(18) U

The University of Texas in Partial Fulfillment

(19) Masters Thesis.

of the Requirements

For the Degree of

Master of Science in Electrical Engineering

THE UNIVERSITY OF TEXAS

(11) August 1963,

PREFACE

This thesis is a theoretical and experimental investigation of the behavior of radio wave propagation, and of a horizontal center-fed half-wave-length dipole antenna, operating in the VHF range near and in the ground. In particular, the effect on the field strength, and the radiation impedance and radiation pattern of the antenna are investigated.

In the event of a nuclear attack, it will be necessary to have communication with civilians in bomb shelters, as well as military requirements for underground communications. With the large number of civilian and military VHF installation that exist, it was considered appropriate to investigate the characteristics of this frequency range in and near ground. Following a brief discussion of some of the previous work in this area, and the general behavior of the earth with regard to frequency, a theoretical discussion is given for relative signal strength and radiation pattern variations with height and depth for a real earth and a perfect conducting earth. Experimental results are then presented and discussed relative to the theoretical calculated values. The experimental measurements were made at frequencies of 179.5 Mc/s and 93.7 Mc/s.

Appreciation is expressed to Air Force Cambridge Research Laboratories for providing the equipment used in the field tests. The assistance of personnel of the Electrical Engineering Research Laboratory, Balcones Research Center, was greatly appreciated. In particular, I wish to thank Professor A. H. LaGrone for his encouragement and for serving

as Supervising Professor in the preparation of this thesis.

Douglas M. Schwartz

The University of Texas

August, 1963

TABLE OF CONTENTS

	Page
I. INTRODUCTION	1
II. THEORETICAL DISCUSSION	3
A. Field Above Ground	5
B. Field Below Ground	11
C. Radiation Patterns	16
D. Summary	20
III. EXPERIMENTAL	21
A. Relative Field Strength	21
B. Radiation Patterns	22
C. Feed-Point Impedance	33
IV. SUMMARY	38
REFERENCES	41
BIBLIOGRAPHY	42
VITA	44

1. INTRODUCTION

Sommerfeld in 1909 considered the problem of radio wave propagation over a spherical earth having finite conductivity. Other scientists and mathematicians worked on the same problem in the following years, but little consideration was given to the problem of radio waves propagating within the earth until the close of World War II. The need for communications with submerged submarines stimulated interest in the problem, and today, the possibility that many activities, both civil and military, may have to go underground because of radiation hazards, again provides a stimulus for investigation in this area.

Some of the major contributors in this field of late have been A. Banos and J. F. Wesley (1953), J. R. Wait (1957), K. G. Budden (1957), A. F. Gangi (1960), and R. K. Moore (1960). The most extensive recent studies were reported by the University of New Mexico Engineering Experimental Station, dealing with the air-sea problem (1961), and the Space-General Corporation, dealing with the air-earth problem (1962). In both of these studies, the frequency range was 10 cps to 10 kcps.

In studying the effects of the earth on radio wave propagation, many complex factors must be considered. The earth, for example, behaves as a conductor at certain frequencies and as a dielectric at others. In between, there is a frequency band where the behavior is not clear cut

and the earth must be treated as an imperfect dielectric. The earth is also nonhomogeneous, so that the conductivity and dielectric constant both vary with soil types, terrain, and moisture content.

In order to provide some information in the VHF range, which includes two important communication bands, FM and TV, this study is made at $f = 93.7 \text{ Mc/s}$ and $f = 179.5 \text{ Mc/s}$. The effects of the earth on the field attenuation and on the radiation impedance and radiation pattern of a half wave dipole in and near the earth are investigated. Horizontal polarization is used.

II. THEORETICAL DISCUSSION

Whether the earth is to be considered a conductor or dielectric depends on the frequency, and, in turn, upon the loss factor $\frac{\sigma}{\omega\epsilon}$.

σ = conductivity in mhos/meter

ϵ = permittivity in farads/meter

ω = radians per second

Figure 1 shows the variation of $\frac{\sigma}{\omega\epsilon}$ with frequency for the terrain types given in Table 1. The criteria for considering the earth as a dielectric or as a conductor are those stated by Krause¹ as given below.

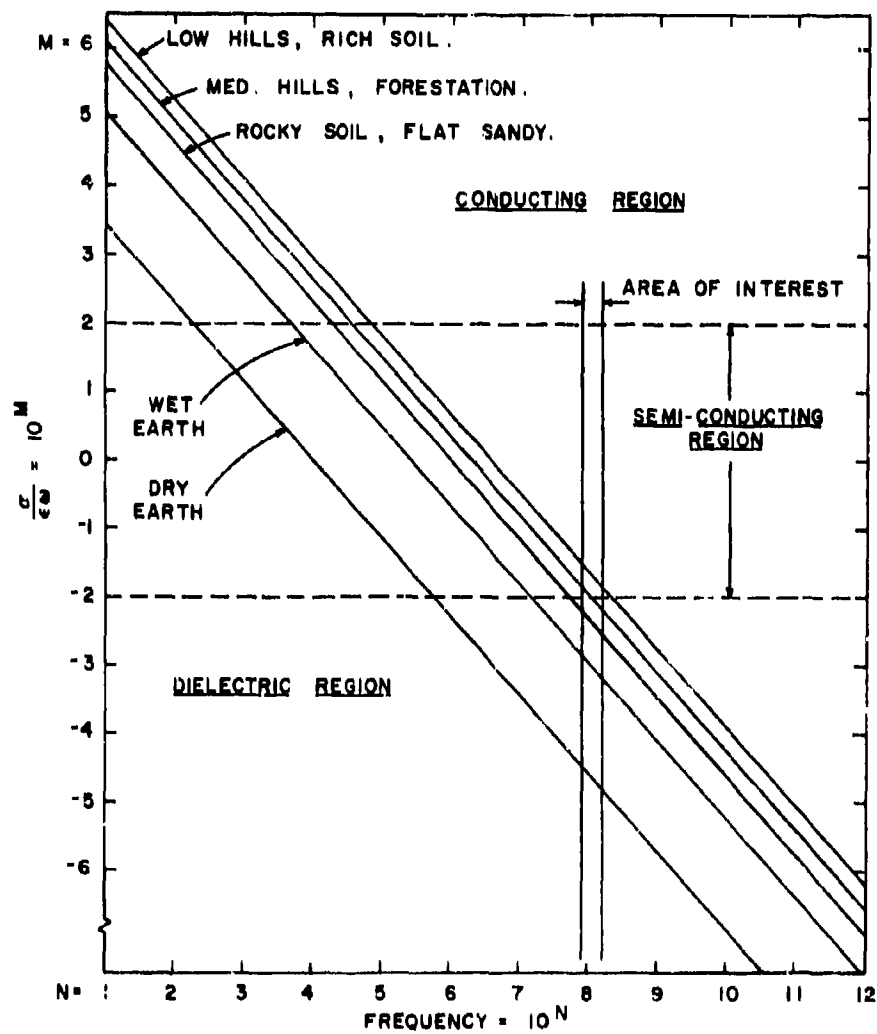
Dielectric: $\frac{\sigma}{\omega\epsilon} < \frac{1}{100}$

Imperfect Dielectric
or Semi-Conductor: $\frac{1}{100} < \frac{\sigma}{\omega\epsilon} < 100$

Conductor: $100 < \frac{\sigma}{\omega\epsilon}$

Table 1

Types of Terrain	Dielectric Constant (relative)	Conductivity (mhos per meter)
Low hills, rich soil ²	20	10^{-2}
Medium hills, forestation	13	0.5×10^{-2}
Rocky soil, flat sandy	10	0.2×10^{-2}
Wet earth ³	10	10^{-3}
Dry earth	5	10^{-5}



RATIO OF $\frac{\sigma}{\epsilon}$ VS. FREQUENCY

FIG. 1.

In the frequency range selected for this study, the VHF range, the earth behaves as a borderline dielectric. Thus, the problem becomes one of analyzing the behavior of the field and of a half wave dipole antenna near the boundary of a perfect dielectric (air) and an imperfect dielectric (earth). Horizontal polarization is assumed.

The geometry of the problem is shown in Figure 2, where $r \gg h > z$. Under these conditions, the field at "r" is assumed to be a plane wave polarized with the E field normal to the plane of incidence. It is further assumed that the path near the receiver is flat, that $\theta_1 = \theta_2$, and angles are constant over the small range that z varies.

A. Field Above Ground

The field above ground at "r + x" can be expressed as:⁴

$$E = E_a e^{-j\beta_x x} \left[e^{j\beta_z z} + \rho e^{-j\beta_z z} \right] \quad (1)$$

where:

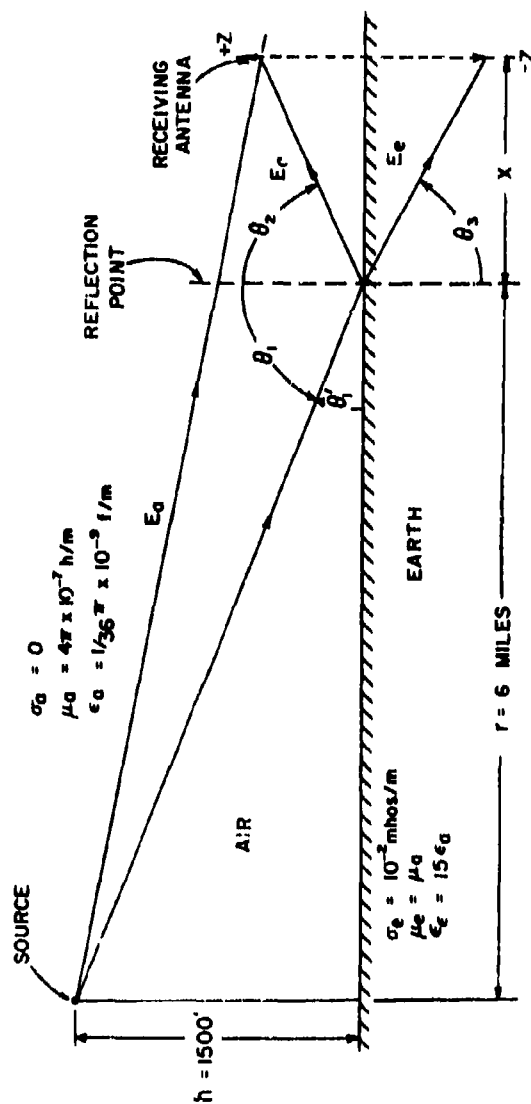
E_a = Incident electric field at r.

$$\beta_x = \frac{\omega}{v_a} \sin \theta_1$$

$$\beta_z = \frac{\omega}{v_a} \cos \theta_1$$

$$v_a = \frac{1}{\sqrt{\mu_a \epsilon_a}} = \text{phase velocity of wave in air.}$$

$$\rho = \frac{z_e - z_a}{z_e + z_a}$$



PROBLEM GEOMETRY

FIG. 2.

Directional impedances in the z direction are

$$\text{for Air: } Z_a = \eta_a / \cos \theta_1$$

$$\text{for Earth: } Z_e = \eta_{ec} \left[1 - \left(\frac{v_e}{v_a} \right)^2 \sin^2 \theta_1 \right]^{-\frac{1}{2}} \quad (2)$$

η_a = intrinsic impedance of the air = 120π .

η_{ec} = complex intrinsic impedance of the earth.

Since the earth is to be treated as an imperfect dielectric, the intrinsic impedance η_e is complex and is given by Ramo-Whinnery as:

$$\eta_{ec} = \frac{\mu_e}{\epsilon_e (1 - j \frac{\sigma_e}{\omega \epsilon_e})} \approx \sqrt{\frac{\mu_e}{\epsilon_e}} \left\{ \left[1 - \frac{3}{8} \left(\frac{\sigma_e}{\omega \epsilon_e} \right)^2 \right] + j \frac{\sigma_e}{2\omega \epsilon_e} \right\} \quad (3)$$

With the following relationships and the fact that $\frac{\sigma}{\omega \epsilon} < 1$, equations (2) and (3) can be combined and simplified.

$$\text{With: } \frac{\eta_e}{\eta_a} = \frac{v_e}{v_a} = \sqrt{\frac{\epsilon_a}{\epsilon_e}} = \sqrt{\frac{1}{k_e}}$$

$$\text{Then: } Z_e \approx \frac{\eta_a}{\sqrt{k_e}} (1 + j \frac{\sigma_e}{2\omega \epsilon_e}) \left(1 - \frac{1}{k_e} \sin^2 \theta_1 \right)^{-\frac{1}{2}} \quad (4)$$

With the original assumption of $r \gg h$, the angle θ_1 approaches 90° and it can be assumed that $\sin^2 \theta_1 \approx 1$. Then

$$Z_e \approx \frac{\eta_a}{\sqrt{k_e - 1}} \left(1 + j \frac{\sigma_e}{\omega \epsilon_0} \right). \quad (5)$$

Using the trigonometric form of the exponentials, equation (1) can be written as:

$$E = E_a e^{-j\beta_x x} \left[(1+\rho) \cos \beta_z z + j(1-\rho) \sin \beta_z z \right] \quad (6)$$

To obtain theoretical values that can be compared with experimental values, the parameters as given in Figure (2) are used.

For 179.5 Mc/s

$$\tan \theta_1' = \frac{1500 \text{ ft}}{6 \text{ miles}}, \quad \theta_1' = 2.7^\circ \quad \text{and} \quad \theta_1 = 87.3^\circ$$

$$\beta_x = \frac{2(1.795)10^8}{3 \times 10^8} = 3.76 \text{ rad/m}$$

$$\beta_z = \frac{2(1.795)10^8}{3 \times 10^8} (0.047) = 0.177 \text{ rad/m}$$

$$Z_a = \frac{377}{0.047} = 7900 \text{ ohms}$$

$$Z_e = \frac{377}{\sqrt{14}} (1 + j 0.067) \approx 100 \angle 3.8^\circ \text{ ohms}$$

$$\text{and} \quad \rho = - \frac{7800 - j 6.6}{8000 + j 6.6}$$

Since the reactive component of ρ in this case contributes little to the magnitude or phase, it will be neglected.

Then $\rho = -0.975$

Substituting these values into equation (5), the expression for E in terms of the variables x and z becomes:

$$E = E_a e^{-j 3.76x} [0.025 \cos(0.177z) + j 1.975 \sin(0.177z)] \quad (7)$$

For 93.7 Mc/s

$$\beta_x = \frac{2(0.937)10^8}{3 \times 10^8} = 1.96 \text{ rad/sec}$$

$$\beta_z = \frac{2(0.0937)10^8}{3 \times 10^8} (0.047) = 0.091 \text{ rad/sec}$$

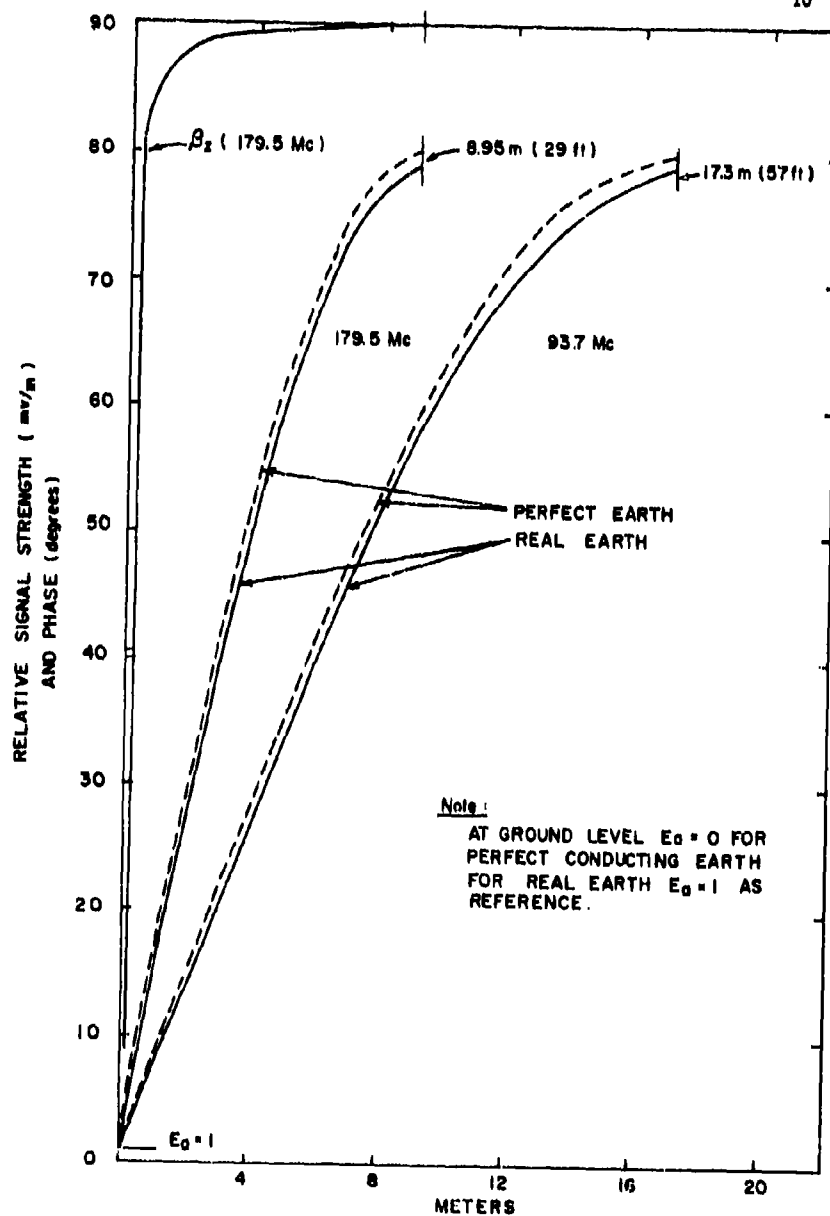
$$Z_a = 7900 \quad Z_e = (377 / \sqrt{14})(1 + j 0.128) \approx 100 / 7.3^\circ$$

$$\rho = \frac{7800 - j 12.8}{8000 + j 12.8} \approx -0.975$$

Then

$$E = E_a e^{-1.96x} [0.025 \cos(0.091z) + j 1.975 \sin(0.091z)] \quad (8)$$

The magnitude and phase of E vs height (z) is shown in Figure 3 with the value of E normalized at the earth's surface. In the vertical plane above ground, E behaves as a standing wave with the first maximum intensity occurring at 8.85 meters (29 ft.) for 179.5 Mc/s and at 17.3 meters (57 ft.) for 93.7 Mc/s. Figure 3 shows only the variation below the first maximum. The electric field and the phase vs height for the earth as a perfect conductor is also shown.



RELATIVE SIGNAL STRENGTH VS HEIGHT

FIG. 3.

The assumption of the earth as a perfect conductor for determining field characteristics above the earth is observed to be good at VHF frequencies.

B. Field Below Ground⁴

The field (E_e) below the ground is the transmitted portion of E_a into the earth. Since the earth is a lossy dielectric, the field will be attenuated as it penetrates into the earth.

Then:

$$E_e = \tau E_a e^{-\gamma_x x} e^{-\gamma_z z}, \text{ where}$$

$$\gamma_z = (\alpha_e + j\beta_e) \cos \theta_3 \quad \gamma_x = (\alpha_e + j\beta_e) \sin \theta_3$$

$$\tau = \frac{E_{z=0}}{E_a} = \frac{2Z_e}{Z_e + Z_a}$$

$$\alpha_e = \omega \sqrt{\frac{\mu_e \epsilon_e}{2} \left(\sqrt{1 + \frac{\sigma_e^2}{\omega^2 \epsilon_e^2}} - 1 \right)}$$

$$\beta_e = \omega \sqrt{\frac{\mu_e \epsilon_e}{2} \left(\sqrt{1 + \frac{\sigma_e^2}{\omega^2 \epsilon_e^2}} + 1 \right)}$$

Using the values of the parameters as given in Figure 2 and previously determined values for Z_e and Z_a , the theoretical field below ground is calculated.

The assumption of the earth as a perfect conductor for determining field characteristics above the earth is observed to be good at VHF frequencies.

B. Field Below Ground⁴

The field (E_e) below the ground is the transmitted portion of E_a into the earth. Since the earth is a lossy dielectric, the field will be attenuated as it penetrates into the earth.

Then:

$$E_e = \tau E_a e^{-\gamma_x x} e^{-\gamma_z z}, \text{ where}$$

$$\gamma_z = (\alpha_e + j\beta_e) \cos \theta_3 \quad \gamma_x = (\alpha_e + j\beta_e) \sin \theta_3$$

$$\tau = \frac{E_{z=0}}{E_a} = \frac{2Z_e}{Z_e + Z_a}$$

$$\alpha_e = \omega \sqrt{\frac{\mu_e \epsilon_e}{2} \left(\sqrt{1 + \frac{\sigma_e^2}{\omega^2 \epsilon_e^2}} - 1 \right)}$$

$$\beta_e = \omega \sqrt{\frac{\mu_e \epsilon_e}{2} \left(\sqrt{1 + \frac{\sigma_e^2}{\omega^2 \epsilon_e^2}} + 1 \right)}$$

Using the values of the parameters as given in Figure 2 and previously determined values for Z_e and Z_a , the theoretical field below ground is calculated.

For $f = 179.5 \text{ Mc/s}$

$$\alpha_e = 2\pi(1.795 \times 10^8) \sqrt{\frac{1}{2(0.774 \times 10^8)^2} \left(\sqrt{1 + (0.067)^2} - 1 \right)}$$

$$\alpha_e = 0.655 \text{ nepers/m}$$

$$\beta_e = 2\pi(1.795 \times 10^8) \sqrt{\frac{1}{2(0.774 \times 10^8)^2} \left(\sqrt{1 + (0.067)^2} + 1 \right)}$$

$$\beta_e = 14.6 \text{ rad/m}$$

$$\cos \theta_3 = \frac{14}{15} = \frac{3.74}{3.88} = 0.964 \quad \theta_3 = 15.4^\circ$$

$$\sin \theta_3 = 0.266$$

$$\tau = \frac{2(100)}{7900 + 100} = 1/40$$

$$\text{Then: } E_e = 1/40 E_a e^{-0.174x} e^{-0.632z} e^{-j3.89x} e^{-j14.1z} \quad (9)$$

For $f = 93.7 \text{ Mc/s}$

$$\alpha_e = 2\pi(0.937 \times 10^8) \sqrt{\frac{1}{2(0.774 \times 10^8)^2} \left(\sqrt{1 + (0.128)^2} - 1 \right)}$$

$$\alpha_e = 0.478 \text{ nepers/m.}$$

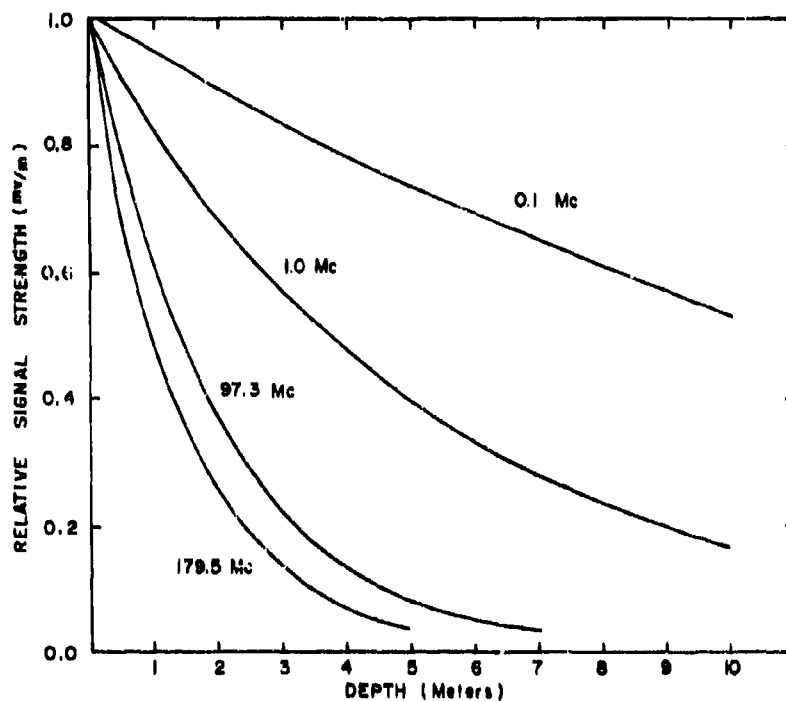
$$\beta_e = 2\pi(0.937 \times 10^8) \sqrt{\frac{1}{2(0.774 \times 10^8)^2} \left(\sqrt{1 + (0.128)^2} + 1 \right)}$$

$$\beta_e = 7.62 \text{ rad/m}$$

$$\text{Then: } E_e = 1/40 E_a e^{-0.125x} e^{-0.462x} e^{-j2.0x} e^{-j.735x} \quad (10)$$

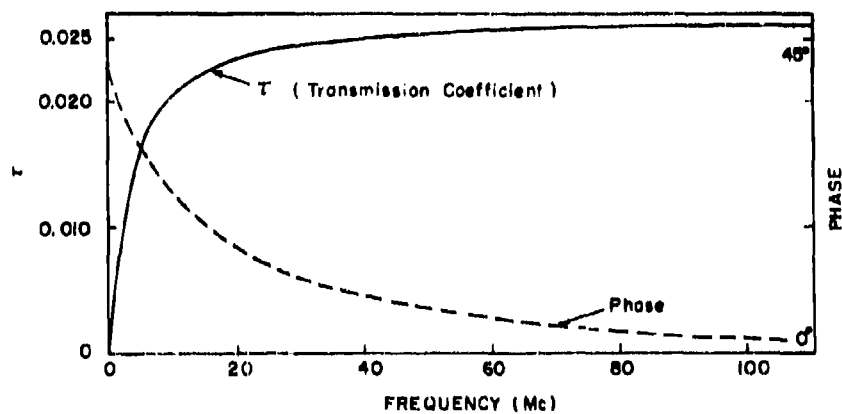
Using equations (9) and (10), the theoretical variation of the relative field strength with depth is plotted in Figure 4a. Also shown is the theoretical variation of 0.1 Mc/s and 1.0 Mc/s signals with depth for comparison purposes. Assuming the field strengths at the ground level to be the same, the strength of the 0.1 Mc/s field at a depth of four meters is found to be approximately eight times that of the VHF field being considered.

In Figure 4b, the theoretical variation of the transmission coefficient with frequency is shown. With the constants that were used for the earth, the transmission coefficient reaches its maximum (0.028) at approximately 93.7 Mc/s and its phase approaches zero. As the frequency approaches zero, the transmission coefficient goes to zero. Consider signals of 0.1 Mc/s and 93.7 Mc/s as having the same incident field strength E_a at a distance (x), then the VHF field strength is approximately fifteen times as great as that of the 0.1 Mc/s field at the earth surface. This is shown in Figure 5. From the above discussion and Figures 4 and 5, it appears that for depths less than five (5) meters, with the same incident field, the VHF frequencies provide greater available field strength due to the larger transmission coefficient.



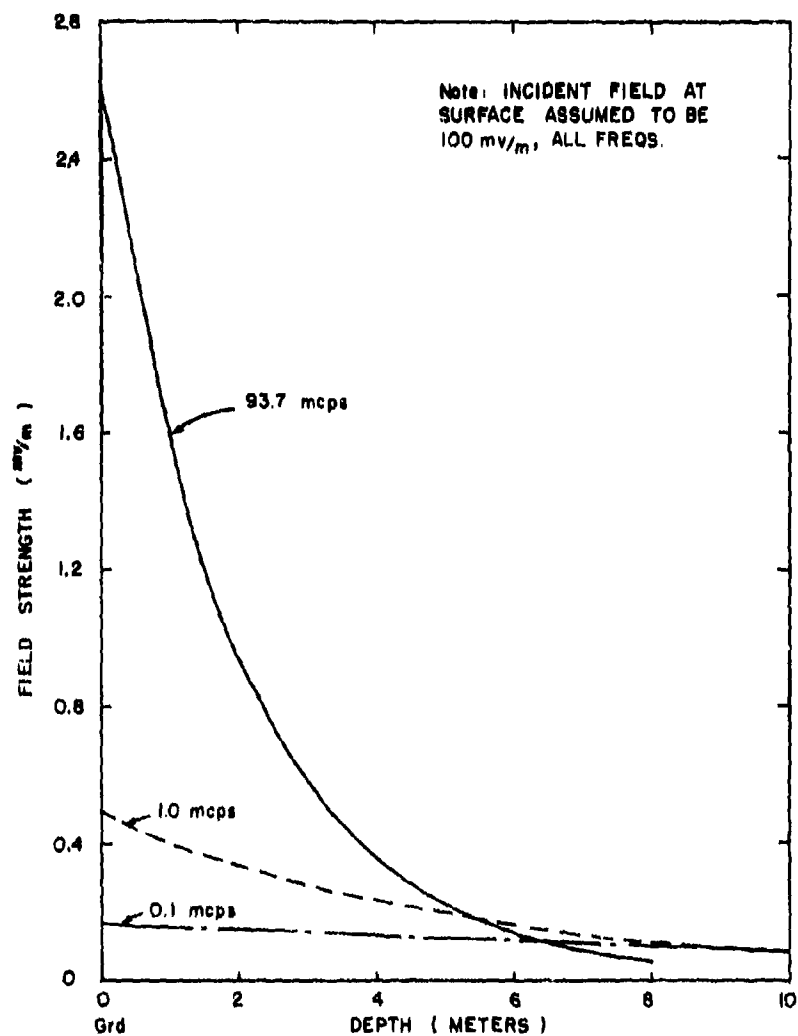
RELATIVE SIGNAL STRENGTH VS. DEPTH

FIG. 4a.



TRANSMISSION COEFFICIENT VS. FREQUENCY

FIG. 4b



FIELD STRENGTH VS. DEPTH

FIG. 5.

C. Radiation Patterns

This discussion is limited to the E-plane, or horizontal pattern, of a half-wave center-fed dipole. The two cases involved, above ground and below ground, are discussed separately.

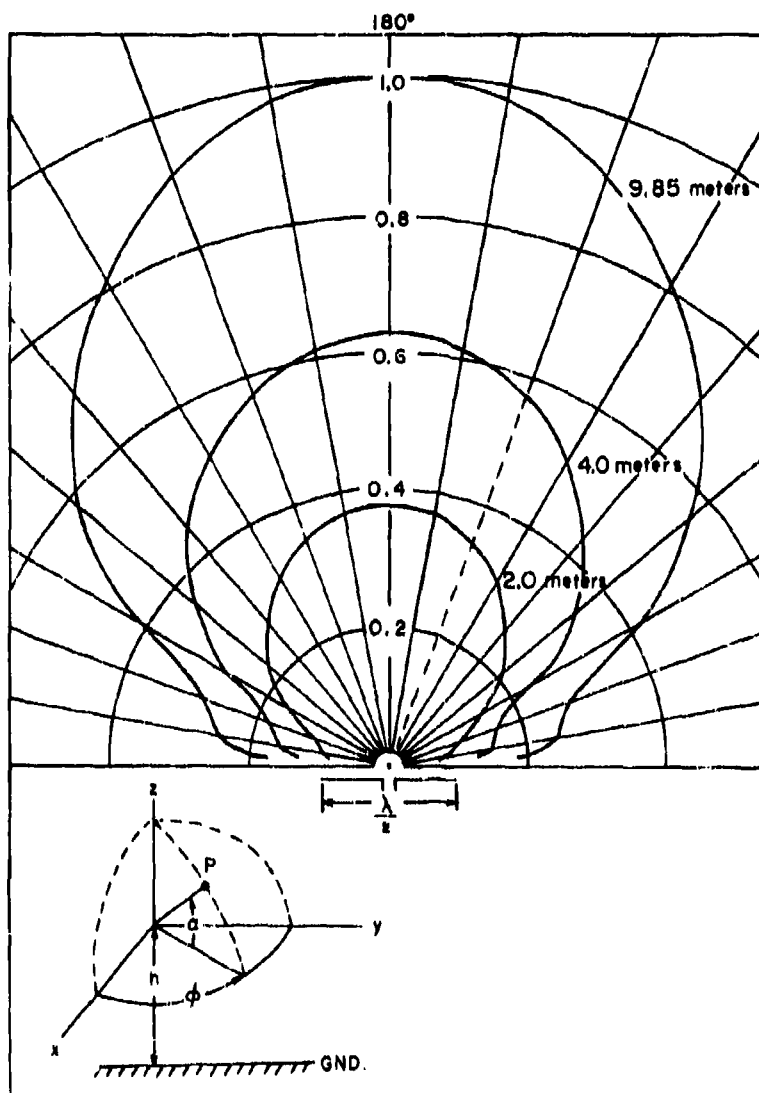
Assuming a perfectly conducting earth, Kraus⁵ has developed an equation for the radiation pattern of a horizontal half-wave dipole above the earth. It is based on treating the problem in the same manner as a two antenna array, where the image antenna is the second antenna. Using this approach, the equation for the field pattern is:

$$E = \left[\frac{\cos \left(\left(\frac{\pi}{2} \right) \cos \phi \cos \alpha \right)}{\sqrt{1 - \cos^2 \phi \cos^2 \alpha}} \right] \sin \left(\frac{2\pi h}{\lambda} \sin \alpha \right) \quad (11)$$

with the geometry as shown on the insert in Figure 6. The factor in brackets represents the field pattern of a dipole in free space, while the second factor is the array pattern. With the spatial angle $\alpha = 2.7^\circ$, a constant in this paper, the second factor is a function of antenna height only, and can be considered constant in the determination of the E-plane pattern of the antenna. The effect of height on the combined signal can be determined by reference to equation (1). Then equation (11) can be written as:

$$E = \left[\frac{\cos \left(\frac{\pi}{2} \cos \phi \right)}{\sin \phi} \right] |K| \quad (12)$$

where K is a function of height and $\cos \alpha \approx 1.0$



RADIATION PATTERN VS. ANTENNA HEIGHT
(FREQUENCY 179.5 Mc)

FIG. 6.

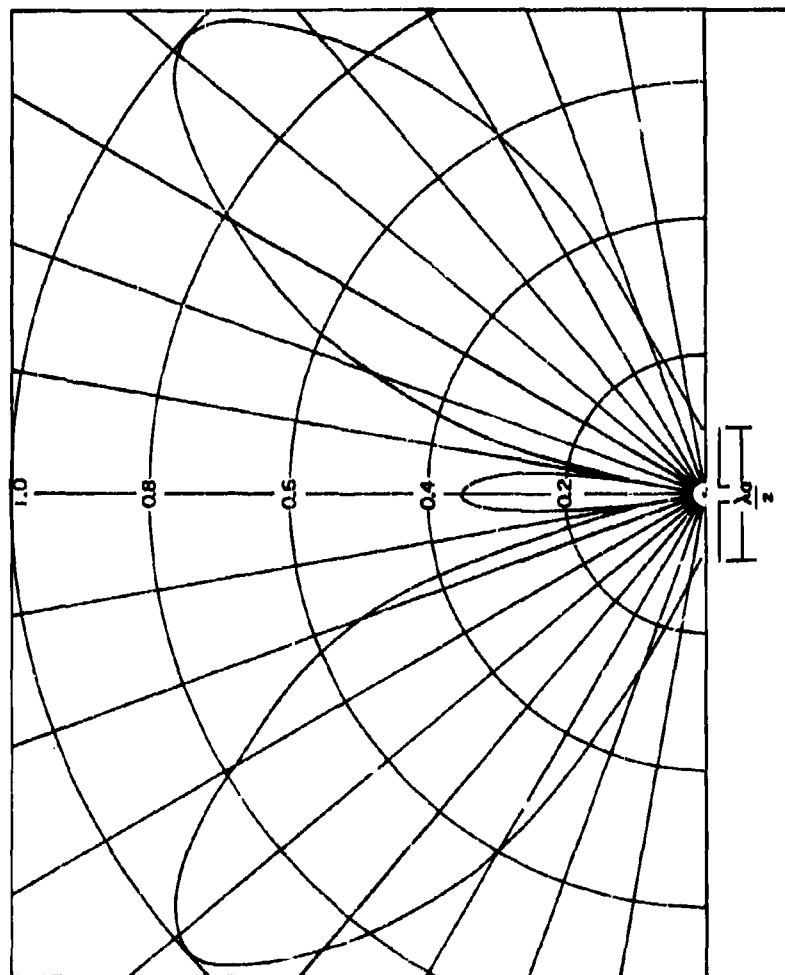
Figure 6 shows the plot of the bracketed term in equation (12), and the previously determined magnitudes as a function of the antenna height factor, K , for heights of 8.95, 4, and 2 meters above local ground.

At ground level, the theoretical analysis of the antenna pattern above a real earth becomes complicated. Since the earth has a finite conductivity and is in contact with the antenna, some antenna current flow into the earth occurs. However, the conductivity of the antenna element is so much greater than that of the earth that essentially all of the current is confined to the antenna. Therefore, the antenna pattern in form at the earth surface is primarily that of a half-wave-length dipole in free space.

Using the parameters as given in Figure 2 for the earth, the velocity of propagation of radio signals in the earth is approximately one-fourth that of air or 0.78×10^8 m/sec. The wavelength of the signal in the earth is likewise reduced to $0.259 \lambda_a$. Therefore, a half-wave-length antenna in air becomes a 1.78 wavelength antenna in the ground. Using the equation developed by Kraus⁶ for the far electric field:

$$E = |E| \frac{\cos (L \cos \phi) / 2 - \cos (L/2)}{\sin \phi} \quad (13)$$

with $\beta = 2\pi/\lambda$ and $L = 1.78\lambda$, the theoretical antenna pattern of a 1.78λ dipole is calculated and shown in Figure 7. This pattern is based on a homogeneous earth with parameters as given in Figure 2, and in shape, is the same as that obtained for a $1.78\lambda_a$ antenna in free space.



RADIATION PATTERN BELOW GROUND
FIG. 7.

An antenna cut to a half-wavelength as measured in the ground, using the constants for the local ground, essentially produces the free-space half-wavelength dipole pattern.

D. Summary

VHF characteristics near the surface of a real earth are not significantly different from VHF characteristics near the surface of a perfect conducting earth. The differences that occur are (1) the maximum field strength for real earth is slightly less due to the reflection coefficient being less than unity, and (2) the field strength at ground level does not go to zero.

Below ground, the VHF refracted field strength is attenuated due to the earth being a lossy dielectric. Radiation patterns are not significantly different from free-space patterns as long as the antenna length is determined from local ground characteristics, and antenna depth is such that boundary conditions at the interface do not affect the pattern. If a receiver system (receiver, transmission lines, antenna) had a system sensitivity of $20\mu\text{v/m}$ across the receiver input terminals, and was five (5) meters (16.4 ft.) deep in the earth, then the incident field strength at the earth surface would have to be 8 mv/m for minimum reception. From this, it is apparent that operation below ground at VHF frequencies requires high transmission powers and short distances. As previously pointed out, for depths less than five (5) meters, the VHF frequency range theoretically does offer greater available field strength than frequencies below 0.1 Mc/s for the same incident field strength, due to the magnitude of the transmission coefficient.

III. EXPERIMENTAL

The experimental work was performed at The University of Texas, Balcones Research Center. The geometry of the path is shown in Figure 2. Two source frequencies were utilized, (1) Channel 7, TV audio at 179.5 Mc/s with average radiated power of 150 kw and (2) FM at 93.7 Mc/s with average radiated power of 94 kw. Both transmitters were on the same tower. The soil conditions at the receiver consisted of a sandy clay to a depth of approximately three feet where a porous rock was encountered.

The receiver system consisted of a General Radio oscillator (1215-B), mixer (874), and IF amplifier (1216-A). The antennas used were center-fed resonant half-wavelength horizontal dipoles.

For: $f = 179.5 \text{ Mc/s}$; antenna length - 77 cm.

$$\frac{\text{Length}}{\text{Diameter}} = \frac{77}{1.5} = 51$$

$f = 93.7 \text{ Mc/s}$; antenna length - 147 cm.

$$\frac{\text{Length}}{\text{Diameter}} = \frac{147}{1.5} = 98.$$

The transmission line from antenna to mixer was 9.66 meters of 50 ohm coaxial cable having an approximate loss of 1 db at both frequencies.

A. Relative Field Strength

In measuring the relative field strength variation with height and depth, a variable length line and tuning stub were inserted at the receiver input for matching purposes. Starting at 1.0 wavelength above ground,

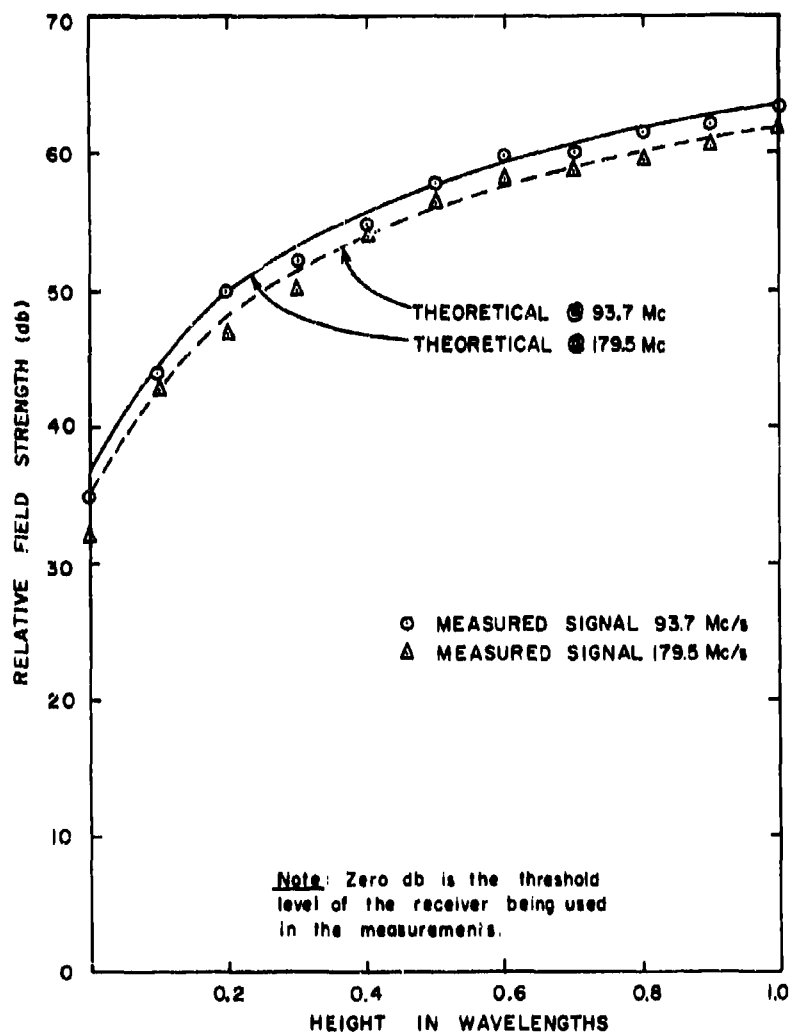
measurements were taken every tenth of a wavelength down to the earth surface at both frequencies. These results are shown in Figure 8.

A study of the curves shows the correlation between the measured data and the theoretical data to be quite good. In the theoretical expression of the reflection coefficient, the term primarily affecting the magnitude of the reflection coefficient is the impedance of the earth (Z_e) which is itself determined by the value selected for the dielectric constant (K_e) of the earth. The value selected for K_e was fifteen (15); however, a value of twenty (20) would have given better correlation with the experimental data.

Figure 9 shows the measured relative field strength variation with distance below the surface of the earth. These measurements were made with an antenna cut to a half wavelength as measured in air. The theoretical variations of the field strength as a function of depth in wavelengths is shown for comparison. Poor agreement between the curves is obvious. The poor agreement is believed to result primarily from the loss of directivity of the antenna cut to a half-wavelength in air when buried in the ground as will be discussed later.

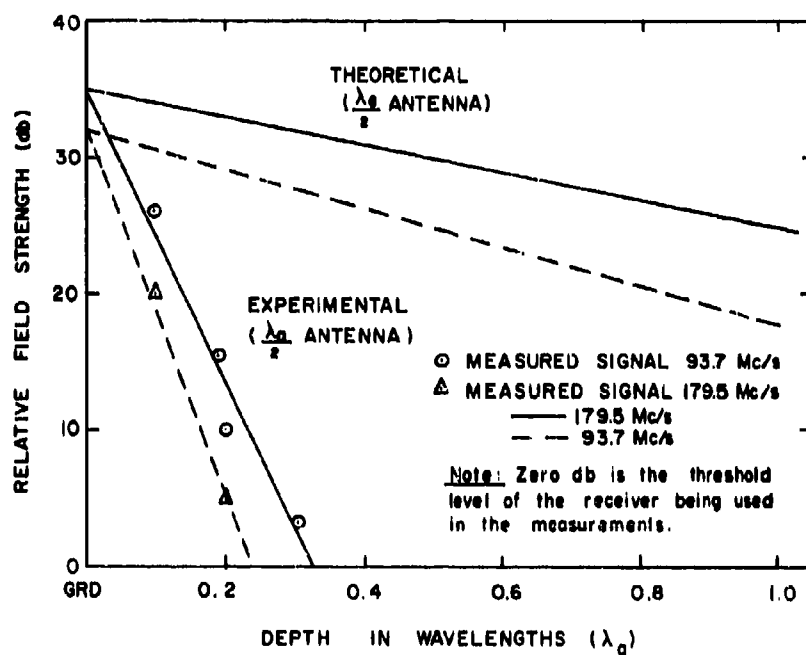
B. Radiation Patterns

The radiation patterns above ground were obtained by rotating the antenna in ten (10) degree increments through 180 degrees of rotation. Since it was expected that the antenna pattern at 1.0 wavelength above



RELATIVE FIELD STRENGTH VS. HEIGHT

FIG. 8.



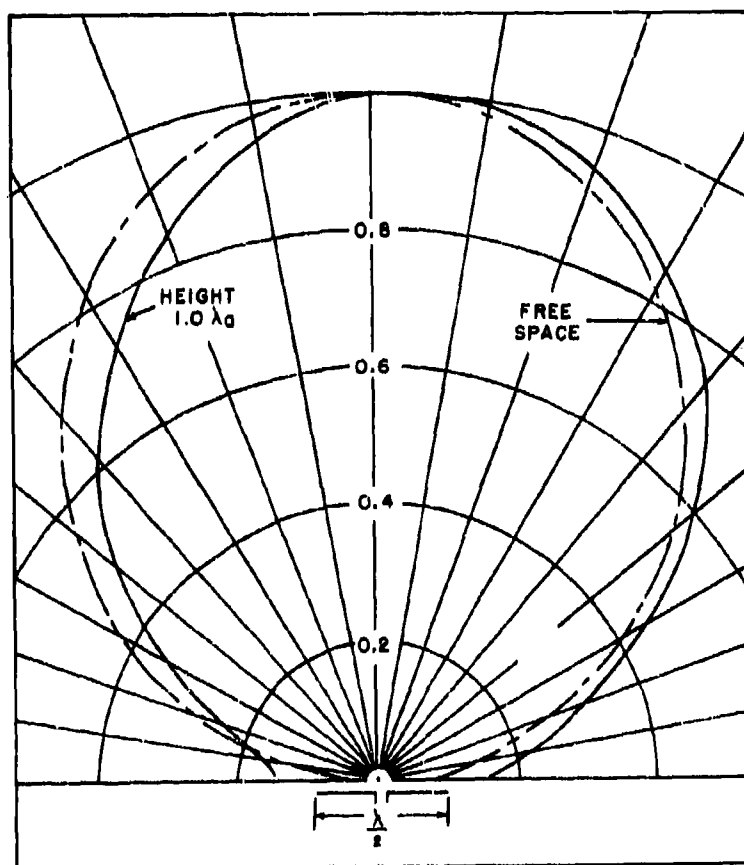
RELATIVE FIELD STRENGTH VS. DEPTH

FIG. 9.

ground would approach the free space pattern, the antenna was first oriented for maximum gain at this height for a reference. No attempt was made to match impedances during these measurements since Terman⁶ states that the radiation resistance, antenna efficiency, directional pattern, and directive gain are not affected by failure to match impedances.

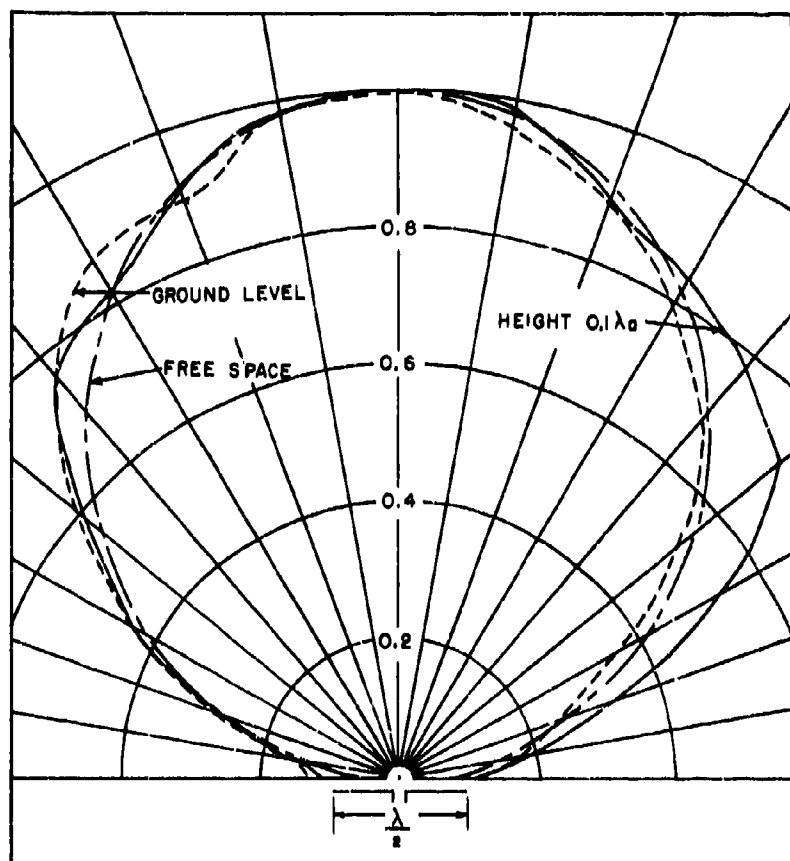
Figure 10 shows the experimental half-wave dipole radiation pattern for 179.5 Mc/s at $1.0\lambda_a$ above ground and the theoretical free space pattern of the same antenna. Since only minor variations in the pattern were obtained from $1.0\lambda_a$ to $0.2\lambda_a$, only the pattern for $1.0\lambda_a$ is shown. Figure 11 shows the patterns at the earth's surface, $0.0\lambda_a$, at $0.1\lambda_a$ and the free space pattern. Figures 12 and 13 show the patterns obtained for the 93.7 Mc/s half wave dipole above ground at the heights indicated. The same measuring procedure is used at 93.7 Mc/s as was used at 179.5 Mc/s. The patterns obtained at $1.0\lambda_a$ above ground at both frequencies compare favorably with the theoretical free space patterns. The deviation in the pattern observed at both frequencies appears to be that of a misalignment of approximately five degrees in the orientation of the experimental patterns.

At ground level, correlation between the theoretical and measured patterns was actually better than expected since difficulty was encountered in keeping approximately the same amount of earth in contact with the antenna as it was rotated in taking the pattern. The same deviation (indenting of the pattern) Figure 11 and Figure 13, occurs at both frequencies, therefore it is not believed to be an error in the measurement of the data. This deviation may be due to one or several obstacles which were present in the test area.



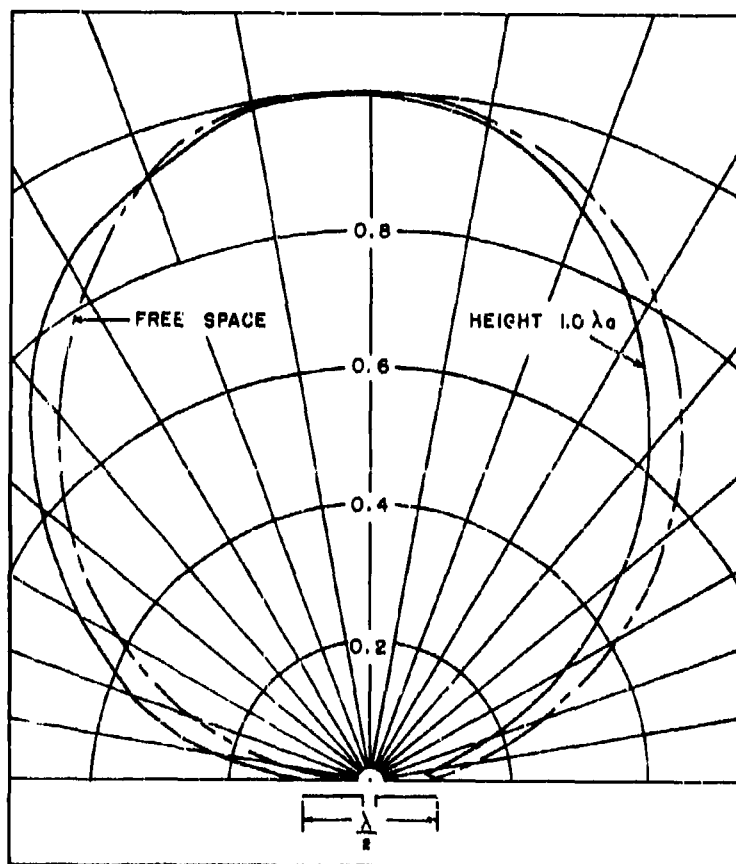
RADIATION PATTERNS AT 179.5 Mc
FROM $1.0 \lambda_0$ TO $0.2 \lambda_0$ ABOVE GROUND

FIG. 10.



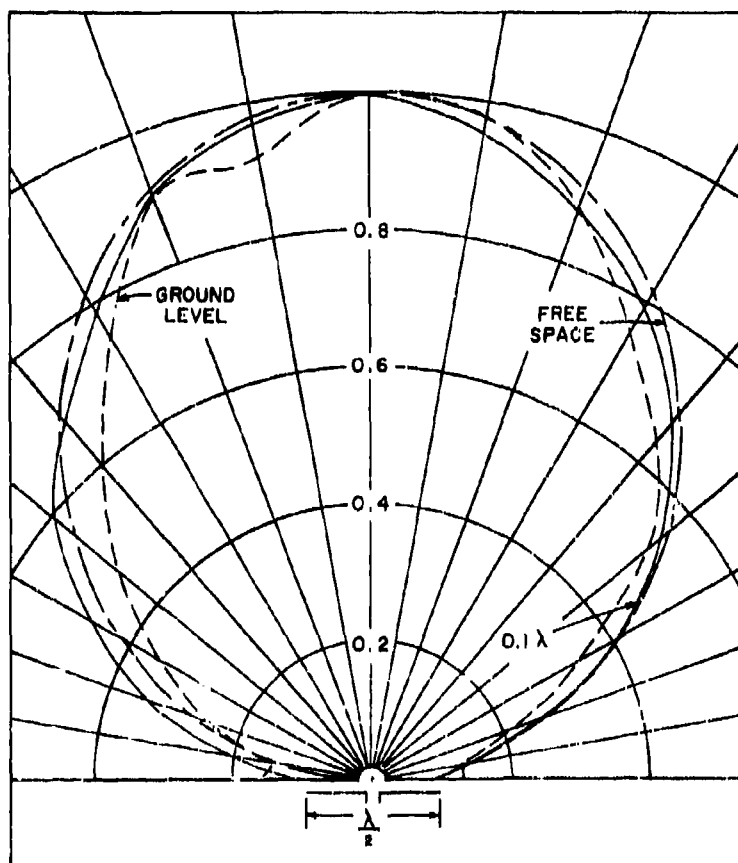
RADIATION PATTERNS AT 179.5 Mc
AT $0.1\lambda_0$ TO $0.0\lambda_0$ ABOVE GROUND

FIG. 11.



RADIATION PATTERNS AT 93.7 Mc
ABOVE GROUND

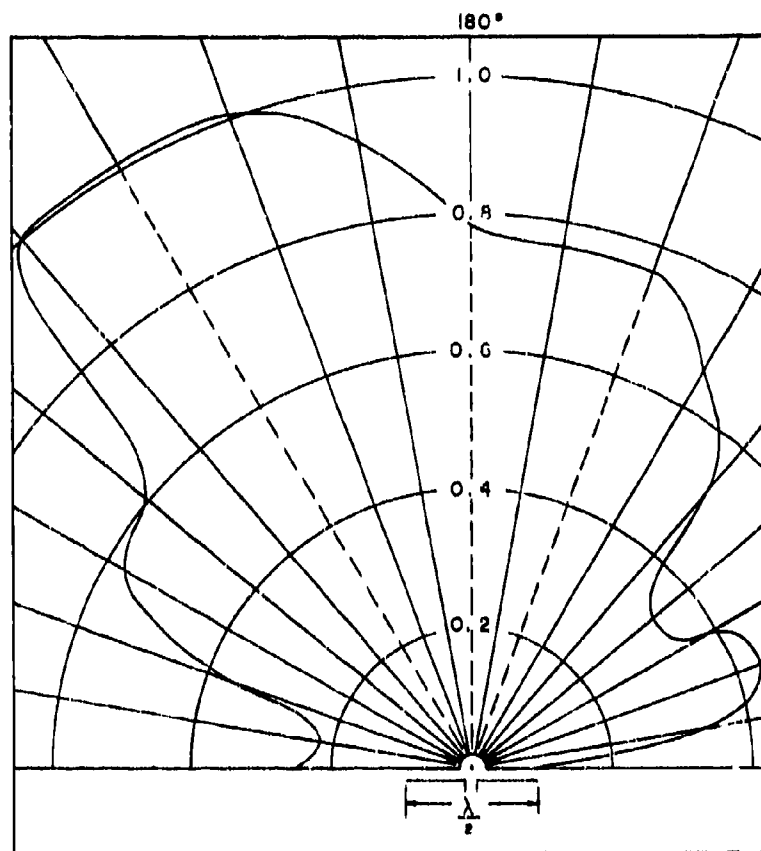
FIG. 12.



RADIATION PATTERNS AT 93.7 Mc
ABOVE GROUND

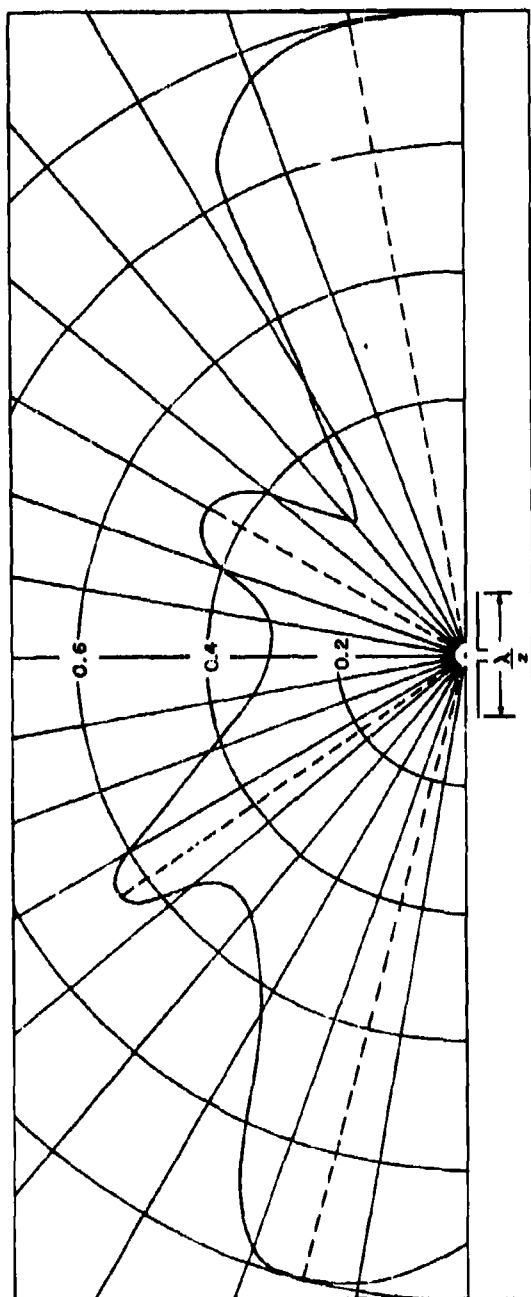
FIG. 13.

A great amount of time was spent in trying different methods of obtaining radiation patterns for underground antennas. Figure 14 shows the radiation pattern obtained at a depth of $0.1\lambda_a$ by rotating the antenna in 10 degree increments. This required burying and digging up the antenna nineteen times. This method is unsatisfactory if for no other reason than the amount of digging required. However, there are other problems involved which make the technique undesirable, such as (1) maintaining a constant depth, (2) keeping the surface above the antenna uniform, (3) keeping the ground cover of the same consistency, and (4) preventing damage to the antenna. Figure 15 shows the radiation pattern obtained at a depth of $0.3\lambda_a$ by moving a small transmitter with a short dipole around the test antenna at a constant radius. This method introduces the problems of maintaining a level and constant height platform for the transmitter, of variations in the soil conditions, and other obstructions below the surface which can not readily be accounted for. However, for the directions indicated by dotted lines in Figures 14 and 15, these relative amplitudes were obtained upon repeated experiments. These patterns show the loss in directivity which partially accounts for the difference between the theoretical signal strength and that obtained experimentally with a $\lambda_a/2$ antenna below ground, as mentioned previously in par. 3A.



RADIATION PATTERN AT $0.1 \lambda_d$ DEPTH
(FREQUENCY 179.5 Mc)

FIG 14 .



RADIATION PATTERN AT $0.3 \lambda_0$ DEPTH
(FREQUENCY 179.5 Mc)

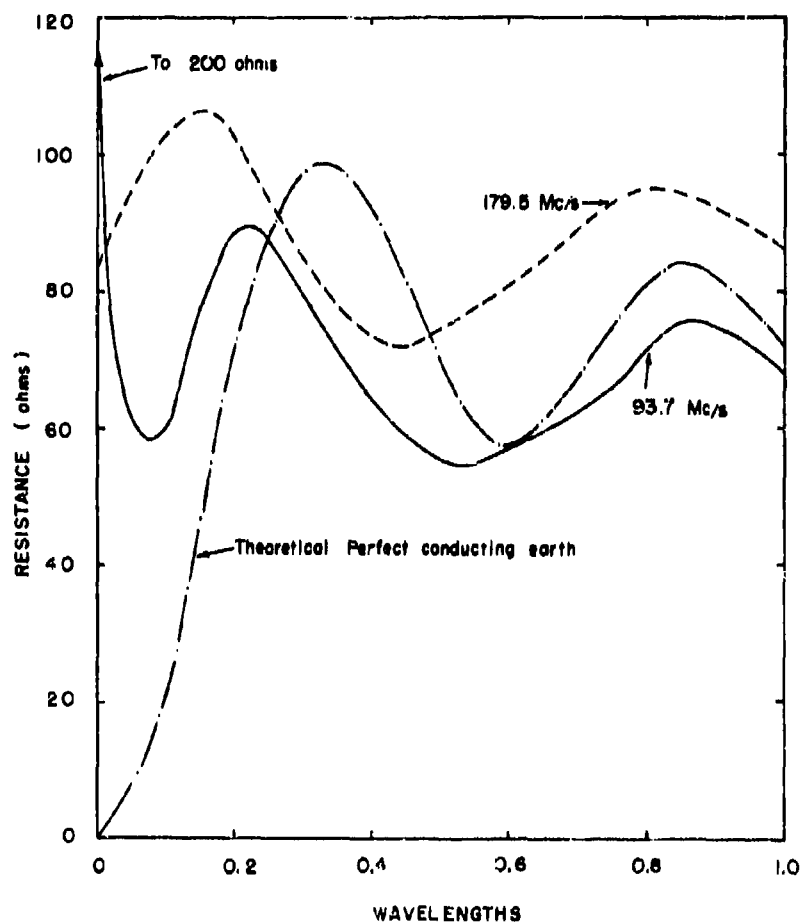
FIG. 15.

C. Feed-Point Impedance

The antenna driving- or feed-point admittance was measured at height intervals of one tenth of a wavelength from a starting height of $1.0\lambda_g$ above ground at both frequencies. The admittance was measured at the receiver end of a coaxial cable connected to the antenna by using a General Radio admittance meter (1602-B). Using a Smith chart and correcting the measured values for the electrical length of the coaxial cable, the impedance at the antenna was determined.

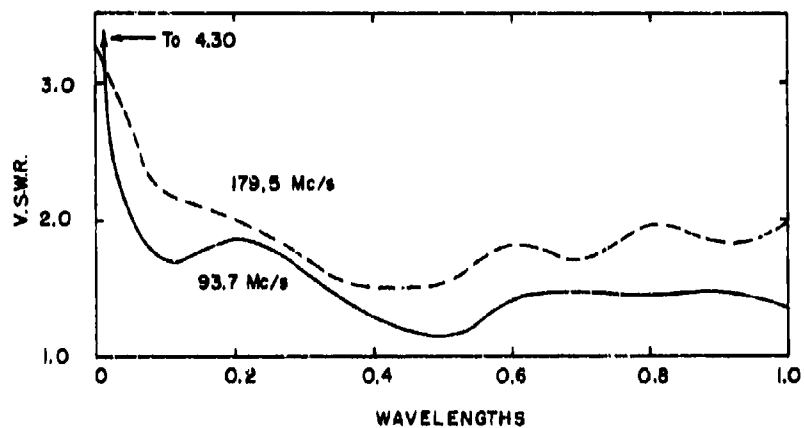
Figures 16 and 17 show the feed-point resistance and reactance, and the standing wave ratio present on the transmission line for the above ground measurements. The theoretical feed-point resistance and reactance for the same measurement heights above a perfectly conducting earth are also shown.

The theoretical values were obtained by assuming an image antenna having the same current distribution and physical characteristics as the test antenna. The feed-point impedance was then obtained by treating the problem as one of two linear center-fed antennas side by side. The original work dealing with this approach was done by P. S. Carter in 1932 and is presented by Kraus⁷ in his text on antennas. Carter's development is for a perfectly conducting earth, with the two antenna current distributions the same. Under these conditions, the theoretical values of the impedance can be obtained easily.

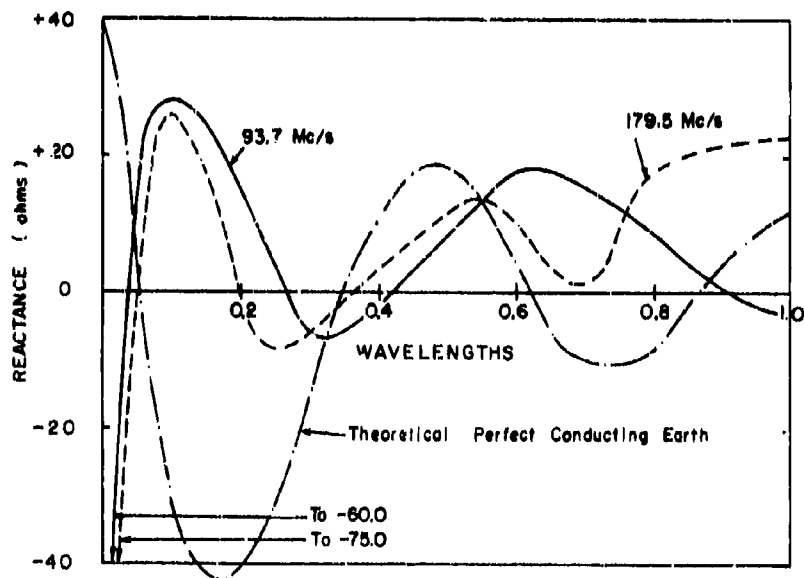


FEED-POINT RESISTANCE VS. HEIGHT

FIG. 16.



STANDING WAVE RATIO VS. HEIGHT



FEED-POINT REACTANCE VS. HEIGHT

FIG. 17.

The method of images is also applicable to the problem involving a real earth, where the current distributions on the subject and image antennas are not the same. In the case of the half wave dipole, the difficulty is in determining the current distribution for the image antenna and expressing it mathematically. The general expression for the voltage at the test antenna terminals⁸ is:

$$V = I_a Z_a + I_i Z_m$$

where:

I_a = the antenna current

I_i = the image current

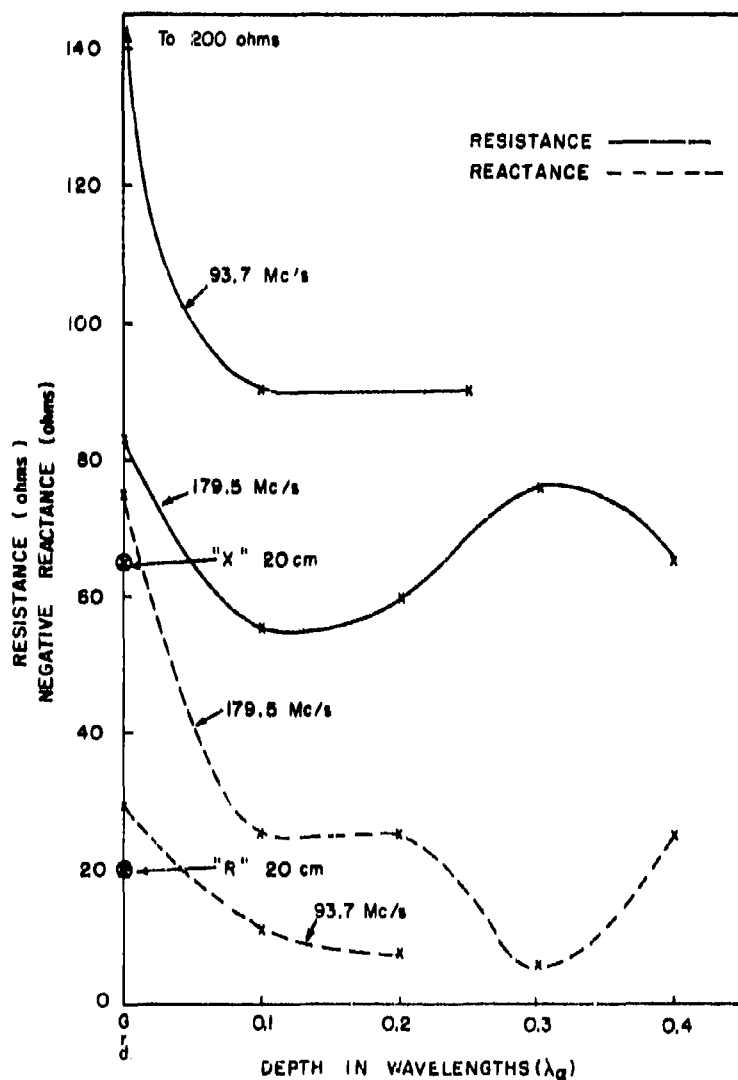
Z_a = self-impedance of the antenna

Z_m = mutual impedance, antenna and its image

and $E = -dV/dz$.

Figure 18 shows the measured impedances below ground for both frequencies. The measurements in these cases were obtained in the same manner as those in the above ground cases. The impedance of an antenna cut to $\lambda_g/2$ is also given at ground level.

From these measurements it is apparent that a considerable variation and mis-match in impedance occurs between the 50 ohm coaxial line and the antenna when the antenna is near the surface of the earth. In the case of the 93.7 Mc/s at the earth surface, the resistive component is approximately two hundred ohms and the mis-match is particularly bad.



FEED-POINT IMPEDANCE VS. DEPTH

FIG. 18.

IV. SUMMARY

(1) The radiation pattern and radiation impedance of a half wavelength dipole at VHF, in and near the ground, have been measured and are reported here.

(2) The variation of the field strength of VHF signals, in and near the ground, have been measured and are reported.

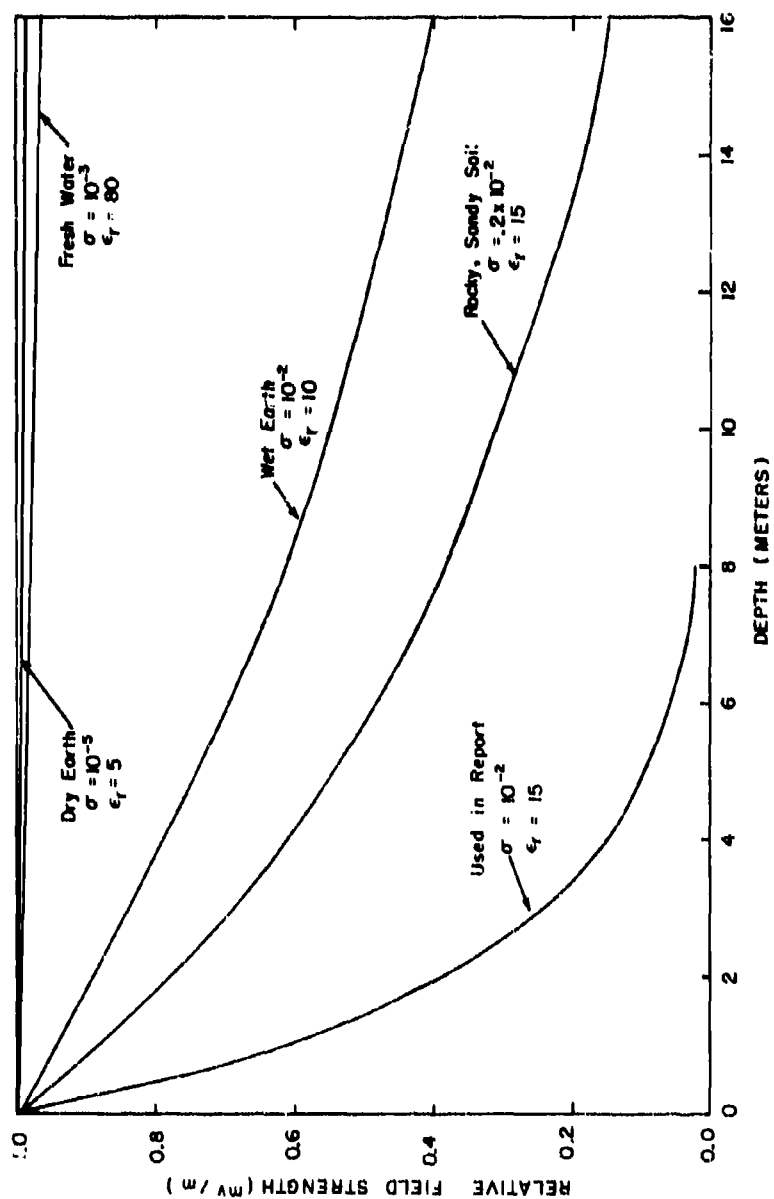
(3) Good correlation was found between the measured and theoretical radiation patterns and field strength variation for above ground conditions.

(4) Theoretically, for the same incident field strength, a larger signal is found for a few feet below the surface of the ground at VHF than at 1.0 Mc/s. The difference in the attenuation and transmission characteristics at these frequencies account for this.

(5) Large variations in the field strength occur for various soil conditions at any given depth. Figure 19 shows this variation for a frequency of 179.5 Mc/s.

The half wavelength dipole appears to be acceptable as an antenna for underground reception, although it does suffer a large loss in capture area when cut to the proper length for local ground conditions.

It appears that a better antenna system than the unshielded dipole used in this study is desirable if one is to take advantage of the available field strength, at VHF, below the earth's surface. Below 1.0 Mc/s considerable investigation of possible antenna systems has been made and some of these may be usable at VHF. As an example, H. A. Wheeler,⁹



RELATIVE FIELD STRENGTH VS. DEPTH
AT 179.5 MC/s
FIG. 19.

PG. 36

40



at 1.0 Mc/s, used a vertical loop in a spherical radome and also a horizontal insulated wire with both ends connected to grounded electrodes.

These antenna systems and other might well be investigated for use at

VHF.



REFERENCES

1. J. D. Kraus, Electromagnetics, McGraw-Hill Book Company, Inc. 1953, p. 392.
2. F. E. Terman, Electronic and Radio Engineering, McGraw-Hill Book Company, Inc., 1955, p. 808.
3. S. Ramo and J. R. Whinnery, Fields and Waves in Modern Radio, John Wiley and Sons, 1960, p. 312.
4. Ibid, reference 3, p. 301.
5. J. D. Kraus, Antennas, McGraw-Hill Book Company, Inc., 1950, pp. 304-308.
6. Ibid, reference 2, p. 900.
7. Ibid, reference 5, pp. 254-268.
8. Ibid, reference 5, p. 304.
9. H. A. Wheeler, "Useful Radiation from an Underground Antenna," Journal of Research of The National Bureau of Standards - D, 65D, No. 1, February, 1961.

BIBLIOGRAPHY

Bronwell, A. B., and Beam, R. E., Theory and Application of Microwaves.

New York: McGraw-Hill Book Company, Inc., 1947.

Bullington, K., "Radio Propagation of Frequencies Above 30 Mc."

Proceedings of the IRE, 35 (October, 1947), 1122.

Bullington, K., "Radio Propagation Variations at VHF and UHF."

Proceedings of the IRE, 38 (January, 1950), 271.

Durram, S. H., "Electromagnetic Fields in the Two Media Caused by Vertical and Horizontal Dipoles in Air." University of New Mexico (Contract Nonr 2798(01)) (September, 1961).

Gangi, A. F., "A Technical Note on Fields from a Buried Horizontal Dipole in a Flat Earth-Flat-Ionosphere System." Space-General Corporation SGC TM 1-10 (March, 1962).

King, R. W. P., The Theory of Linear Antennas. Cambridge: Harvard University Press, 1956.

King, R. W. P., and Harrison, C. W., Jr., "Half Wave Cylindrical in a Dissipative Medium." Journal of Research, National Bureau of Standards, 64D, No. 4 (July, 1960), 365-380.

Kraus, J. D., Antennas. New York: McGraw-Hill Book Company, Inc., 1950.

Kraus, J. D., Electro-Magnetics. New York: McGraw-Hill Book Company, Inc., 1953.

- Moore, R. K., and Blair, W. E., "Dipole Radiation in a Conducting Half-Space." Journal of Research, National Bureau of Standards, 65D, (November, 1961).
- Ramo, S., and Whinnery, J. R., Fields and Waves in Modern Radio. New York: John Wiley and Sons, 1960.
- Stratton, J. A., Electromagnetic Theory. New York: McGraw-Hill Book Company, Inc., 1941.
- Terman, F. E., Electronic and Radio Engineering. New York: McGraw-Hill Book Company, Inc., 1955.
- Wheeler, H. A., "Useful Radiation from an Underground Antenna," Journal of Research of the National Bureau of Standards-D, Radio Propagation, 65D, No. 1 (February, 1961).
- Williams, R. H., "Propagation Between Conducting and Nonconducting Media." University of New Mexico (Contract Nonr 2798 (01), (September, 1961).